POLITECNICO DI TORINO
Repository ISTITUZIONALE

Automated Multicohort Mobility Assessment With an Instrumented L-Test (iL-test)

(Article begins on next page)

14 August 2025

Automated Multicohort Mobility Assessment With an Instrumented L-Test (iL-test)

Jose Albites-Sanabria, *Member, IEEE*, Pierpaolo Palumbo, Ilaria D'Ascanio, Tecla Bonci, Marco Caruso, *Member, IEEE*, Francesca Salis, Andrea Cereatti, *Member, IEEE*, Silvia Del Din, *Member, IEEE*, Lisa Alcock, Arne Kuederle, Anisoara Paraschiv-Ionescu, Eran Gazit, Felix Kluge, Cameron Kirk, M. Encarna Micó-Amigo, Kirsty Scott, Clint Hansen, Jochen Klenk, Lars Schwickert, Dimitrios Megaritis, Ioannis Vogiatzis, Clemens Becker, Walter Maetzler, Jeffrey M. Hausdorff, Brian Caulfield, Beatrix Vereijken, Lynn Rochester, Arne Muller, Claudia Mazzà, Ilaria Carpinella, Thomas Bowman, Roberta De Ciechi, Alessandro Torchio, Davide Cattaneo, Simona Bianchi, Maurizio Ferrarin, *Senior Member, IEEE*, Pericle Randi, Lucrezia Piraccini, Angelo Davalli, Lorenzo Chiari, and Luca Palmerini

Abstract—**The L-test is a performance-based measure to assess balance and mobility. Currently, the primary outcome from this test is the time required to finish it. In this study we present the instrumented L-test (iL-test), an L-test wherein mobility is evaluated by means of a wearable inertial sensor worn at the lower back. We analyzed data from 113 people across seven cohorts: healthy adults, chronic obstructive pulmonary disease, multiple sclerosis, congestive heart failure, Parkinson's disease, proximal femoral fracture, and transfemoral amputation. The iL-test automatic segmentation was validated using stereophotogrammetry. Univariate and multivariate analyses were performed on 164 kinematic features derived from inertial signals to identify distinct patterns across different cohorts. The iL-test accurately recognized and segmented activities during the L-test for all cohorts (technical validity). A random forest classifier revealed that proximal femoral fracture and transfemoral amputation induced significantly different mobility patterns compared to healthy people with AUC values of 0.89 and 0.99, respectively. Strong correlations were found between kinematic features and clinical scores in multiple sclerosis, congestive heart failure, proximal femoral fracture, and transfemoral amputation, with consistent patterns of decreased movement ranges and smoothness with increasing disease severity. Furthermore, features derived from 90° and 180° turns were found to be important contributors to differentiation amongst cohorts, underscoring the need to evaluate different turn degrees and directions. This study emphasizes the iL-test potential to deliver automated mobility assessment across a wide range of clinical conditions, indicating a prospective avenue for improved mobility assessment and, eventually, more informed healthcare interventions.**

Index Terms—**Mobility, wearable sensors, objective measurements.**

I. INTRODUCTION

MOBILITY, the capacity to move, transition, and navigate one's environment, is fundamental to human independence and well-being [1]. It reflects our ability to engage with the world, interact with our surroundings, and maintain a good quality of life. Yet, it is a facet of health that often goes unnoticed until compromised by injury, chronic conditions, or age-related syndromes [2], [3].

To assess mobility comprehensively in clinical populations, healthcare professionals have traditionally relied on clinical questionnaires and tools to measure functional mobility, such as the Timed Up and Go (TUG) test [4]. The TUG test,

a concise yet informative assessment, requires individuals to rise from a seated position, walk a short distance, perform a 180° turn, and return to a seated position. The score is represented by the time taken to perform the test, usually measured with a stopwatch. It is a valuable tool for clinicians, offering quick insights into an individual's mobility and fall risk [5]. The use of wearable technology such as inertial sensors allowed the development of the instrumented TUG (iTUG), which has been used in various studies in the past years [6] to enable analyses of the quality of the movements performed during the TUG assessment. Research using the iTUG has demonstrated the clinical relevance of sensor-derived variables in predicting fall risk and diagnosing mobility impairments [6], [7]. These findings highlight the importance of incorporating inertial sensor-based analyses into mobility assessments, providing a strong rationale for extending their application to the L-test.

In 2005, Deathe and Miller [8] introduced the L-test as a variation of the TUG test, designed to overcome the ceiling effect of the TUG found in higher-functioning individuals. The first proposers of the L-test indicated that when assessing a patient's gait during clinical examinations, clinicians usually asked the patient to get up and walk out of the room, turn 90° and go down the hall, then return to the room and sit down. This walking path, representing an "L" configuration, required turns to both the right and the left. In fact, in real-world conditions, one should be prepared to perform several turns in different directions and angles. Comprised of turns in both directions and at 90° and 180°, the L-test might provide a more comprehensive and detailed evaluation of an individual's mobility status, making it a promising platform for in-lab advanced mobility assessment.

Over the past 10 years, several studies have confirmed the L-test as a reliable, objective tool for assessing walking ability in different populations [9], [10], [11], [12] and a recent study [13] validated an algorithm to segment activities during an L-test in 20 healthy adults. However, no studies have been found to incorporate inertial sensors to analyze kinematics features during the L-test in different clinical populations. This study introduces the instrumented L-test (iL-test) as a novel mobility assessment tool and evaluates its feasibility for extracting digital mobility outcomes (DMOs) that are both technically valid and clinically informative across diverse clinical cohorts. We achieve this through: (1) technical validation of the automatic segmentation of the iL-test through comparison with stereophotogrammetry as the gold standard; (2) discriminant validation, assessing the feasibility of sensor-derived kinematic features to potentially differentiate between cohorts; and (3) construct validity, evaluating the clinical relevance of these kinematic parameters by correlating them with established clinical scales.

II. MATERIALS AND METHODS

A. Study Design and Participants

The study included two distinct datasets: the Technical Validation Study dataset (TVS) of Mobilise-D and the MOTU dataset. In the Mobilise-D dataset, a convenience sample of 100 adults from six different cohorts was analyzed: healthy

adults (HA), chronic obstructive pulmonary disease (COPD), multiple sclerosis (MS), congestive heart failure (CHF), Parkinson's disease (PD), and proximal femoral fracture (PFF). Participants were recruited at five sites: the Newcastle upon Tyne Hospitals NHS Foundation Trust and the Sheffield Teaching Hospitals NHS Foundation Trust, UK (ethics approval granted by the London-Bloomsbury Research Ethics Committee, 19/LO/1507); Tel Aviv Sourasky Medical Center, Israel (ethics approval granted by the Helsinki Committee, Tel Aviv Sourasky Medical Center, Tel Aviv, Israel, 0551-19TLV); Robert Bosch Foundation for Medical Research (ethics approval granted by the ethical committee of the medical faculty of The University of Tübingen, 647/2019BO2) and University of Kiel, Germany (ethics approval granted by the ethical committee of the medical faculty of Kiel University, D438/18). All participants gave written informed consent to take part in the study. Additional information about the TVS protocol can be found in [14], [15], and [16].

The MOTU dataset consisted of 13 transfemoral amputees (TFA) recruited by the MOTU project in two clinical sites: the INAIL Prosthesis Centre, Budrio, Italy (ethics approval granted by CE AVEC, 537/2019/OSS/AUSLBO) and the Palazzolo Institute of the Don Gnocchi Foundation, Milan, Italy (ethics approval granted by the IRCCS Fondazione Don Carlo Gnocchi Ethics Review Board, 08_16/10/2019). The study was conducted following the ethical principles for medical research expressed in the Declaration of Helsinki. Written informed consent was obtained from all participants.

B. Experimental Protocol

In the test, the participant was asked to sit in a chair, stand up, walk straight, turn 90° around a mark, walk straight to the second mark, make a 180° turn, walk straight to the first mark, make a final 90° turn, and return to the chair to sit down (supplementary video).

The participants performed the L-test while wearing an inertial sensor on the lower back. In Mobilise-D, the L-test was made of two arms 4m × 2m, and the inertial sensor was a Dynaport MM+ (McRoberts, the Netherlands) (sampling frequency 100 Hz, triaxial acceleration range: ±8g, resolution: 1 mg; triaxial gyroscope range: ±2000°/s, resolution: 0.07 °/s). In MOTU, the L-test was made of two arms 7m × 3m, and the inertial sensor was from the mTest3 functional assessment suite (mHealth Technologies, Bologna, Italy) (sampling frequency 100 Hz, triaxial acceleration range: ±2g, resolution: 0.06 mg; triaxial gyroscope range: ±250°/s, resolution: 0.0076 °/s). The Mobilise-D used a reduced distance version of the test due to constraints of the stereophotogrammetry systems at some of the clinical sites. To ensure consistency in the analysis, metrics directly sensitive to path length, such as total walking duration, were excluded from comparisons (see Table III).

C. L-Test Segmentation Algorithms

The L-test was segmented into six subphases: Sit-to-Walk (StW), Walking (W), three turns comprised of a first 90° turn (T1), followed by a 180° turn (T2) and a second 90° turn (T3), and Turn-To-Sit (TtS). Figure 1 presents an example of the inertial signals recorded during an instrumented L-test.

TABLE I
PARTICIPANTS' CHARACTERISTICS (MEAN ± SD)

	HA (n = 20)	CHF (n = 10)	COPD (n = 17)	MS (n = 19)	PD (n = 19)	PFF (n = 15)	TFA (n=13)
Study			Mobilise-D				MOTU
Age (years)	71.7 ± 5.8	68.8 ± 12.6	69.4 ± 9.1	47.6 ± 8.4	69.8 ± 7.3	81.5 ± 8.2	57.8 ± 20.8
Height (m)	1.66 ± 0.10	1.75 ± 0.10	1.69 ± 0.07	1.70 ± 0.13	1.74 ± 0.06	1.70 ± 0.09	-
Weight (kg)	75.1 ± 11.8	86.1 ± 15.8	73.7 ± 14.2	84.5 ± 23.5	78.0 ± 14.7	69.5 ± 15.5	64.1 ± 14.3
Sex (M/F)	11/9	7/3	9/8	10/9	16/3	9/6	11/2
LLFDI	73.5 ± 14.2	72.3 ± 19.7	59.1 ± 8.0	57.5 ± 10.9	60.7 ± 12.6	58.1 ± 14.2	-
KCCQ	-	82.2 ± 21.5	-	-	-	-	-
FEV-1	-	-	56.8 ± 19.2	-	-	-	-
EDSS	-	-	-	3.6 ± 1.7	-	-	-
UPDRS-III	-	-	-	-	27 ± 12.5	-	-
SPPB	-	-	-	-	-	7.5 ± 3.3	-
AMP	-	-	-	-	-	-	32.9 ± 7.9

LLFDI: Late Life Function and Disability Instrument; KCCQ: Kansas City Cardiomyopathy Questionnaire; FEV-1: forced expiratory volume in one second (expressed as a percentage of the predicted norm); EDSS: Expanded Disability Status Scale; UPDRS-III: Unified Parkinson's Disease Rating Scale Part III; SPPB: Short Physical Performance Battery; AMP: Amputee Mobility Predictor.

State-of-the-art algorithms were applied to identify each of the segmented phases of the L-test. An adapted version of the Adamowicz algorithm was used to identify standing and sitting transfers. The algorithm identifies postural transfers based on the convolutional wavelet transform of the acceleration norm [17]. An adapted version of the El-Gohary algorithm was used to identify turn segments using a peak identification procedure on the angular velocity around the vertical axis [18]. We used two gait sequence detection algorithms (GSD A and GSD B) to identify the walking phase based on the acceleration signal [19]. GSD A was applied to cohorts with faster walking speeds (HA, CHF, COPD), and GSD B was applied to those with slower walking speeds (MS, PD, PFF, TFA). A last block, named 'state-machine logic', was applied after identifying all events. This block corrected any overlap between two consecutive identified events based on the logical succession of the L-test sub-phases. Figure 2 details the steps followed in the L-test segmentation. Supplementary Table 1 details the signal preprocessing required for each of the described algorithms.

We validated the segmentation according to the logical criteria shown in Table II. A segmentation (true or false) was considered successful if all sub-phases were correctly identified. For the three turns during walking (C3), additional conditions were tested to verify that each of the turns was congruent with the path of the L-test. Validation = C1 & C2 & C3 & C4, where C3 = C3.1 & C3.2 & C3.3 & C3.4 & C3.5.

Moreover, a second validation procedure was applied to the cohorts of the Mobilise-D dataset. Stereophotogrammetry was used as a reference system [20] to establish the accuracy of walking and postural transfer algorithms. In Figure 3, the dashed vertical lines mark the postural transfer and gait events identified by the iL-test segmentation algorithm. A Sit-to-Walk
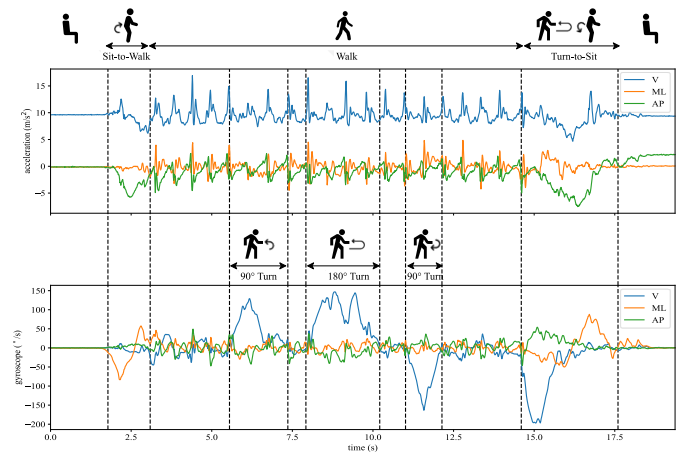
Fig. 1. Recorded sensor signals (V: vertical, ML: mediolateral, AP: anteroposterior) during the iL-test: triaxial acceleration [m/s2] (upper) and angular velocity [°/s] (lower). The black dashed vertical lines segment the task.
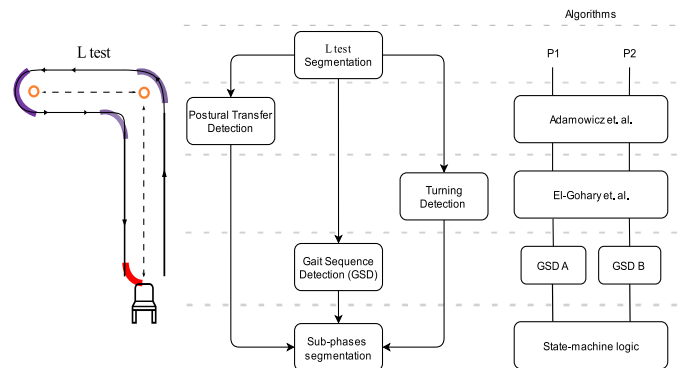
Fig. 2. L-test segmentation algorithm. Left: L-test path, purple highlights the three turns to be identified while walking; red highlights the Turn-To-Sit (TtS) segment. Middle: Instrumented L-test segmentation flow. Right: Algorithms used in the identification of each of the phases. GSD A was applied to P1: HA, COPD, and CHF, and GSD B to P2: MS, PD, PFF, and TFA.

TABLE II
L-TEST LOGICAL VALIDATION FOR CORRECT SEGMENTATION

Conditions	Sub-Phases	Outcome
C1	1 Sit-to-Walk	0/1
C2	1 Walking	0/1
C3	Turns during walking	0/1
C4	1 Turn-to-Sit	0/1
Sub-conditions	Description	Outcome
C3.1	3 turns identified	0/1
C3.2	First turn around 90° ([60°-120°])	0/1
C3.3	Second turn around 180° ([150°-210°])	0/1
C3.4	Third turn around 90° ([60 -120])	0/1
C3.5	First and Third turn in opposite directions	0/1

was obtained by merging a Sit-to-Stand with the start of a gait segment. Processed information from stereophotogrammetry was used to get the initial and end walking segments. For the validation of postural transfers, the start and end of standing and sitting were derived from the vertical axis of the raw stereo signal from the lower back. An automatic algorithm identified the vertical displacement by finding peaks on the derivative of this signal (Figure 3, bottom).
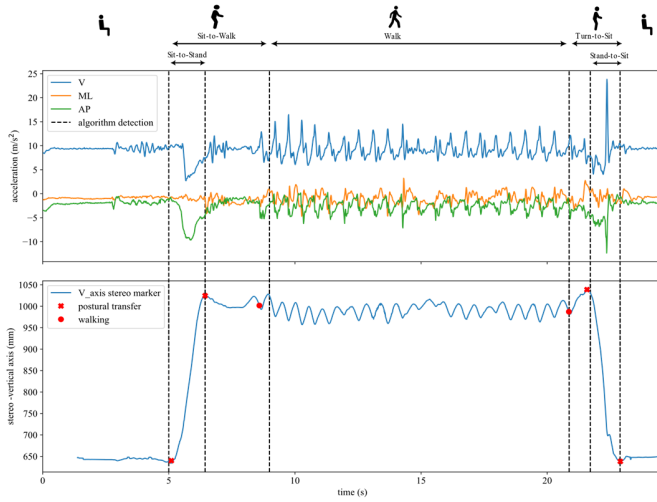
Fig. 3. Validation of the L-test segmentation against stereophotogrammetry. Accelerometer signals (upper) and raw vertical stereo signal from a marker at the lower back (bottom). Black dashed vertical lines indicate the start and end of the algorithm-identified events. Red marks indicate the start and end of the gold standard segments derived from the stereophotogrammetric system.

The mean absolute error (MAE) between the gold standard and the iL-test algorithms at the start and end of each postural transfer and gait segment was computed to assess the accuracy of our proposed method in identifying and segmenting the phases within the L-test. In addition to MAE, the Jaccard index [21] was calculated to evaluate the similarity between the algorithm's segmentation and the gold standard. The Jaccard index measures the intersection over the union of two sets, providing a metric that quantifies the percentage of overlap between the identified and true segments.

D. Kinematic Parameters

A set of 164 kinematic features was extracted for each participant during the L-test. These features included durations, ranges, and smoothness, offering a comprehensive view of mobility (Table III). These features were extracted from triaxial accelerometer and gyroscope signals independently depending on the property analyzed. Stride length and speed calculations integrated both accelerometer and gyroscope data. Accelerometer and gyroscope signals were low-pass filtered with a 5 Hz, 4th order Butterworth filter. These features were selected conveniently to match with features used in previous instrumented tests, such as the iTUG [6], [22], [23], [24]. The duration of the walk sub-phase was not considered as it is sensitive to the path length of the L-test, which differed between cohorts.

In this article, a specific kinematic parameter is identified by its corresponding sub-phase abbreviation, followed by the type of feature, sensor, and the axis to which it applies. For example, the normalized jerk score of the gyroscope in the vertical axis during the second turn, is named T2-NJS GyroV.

E. Statistical Analyses

We explored the differential distribution of the kinematic features among the cohorts with univariate and multivariate

TABLE III
FEATURES EXTRACTED FROM EACH SENSOR, SUB-PHASE OF THE INSTRUMENTED L-TEST

Feature	Sensor	(Sub)Phases	Description
Duration [s]	Accelerometer, Gyroscope	Sit-to-Walk, Turns, Turn-to-Sit	Duration of each subphase of the L-test
Cadence [steps/min]	Accelerometer	Walking	Number of steps within a minute (min) estimated in each walking bout. CAD A [22] was applied for P1 and CAD B [23] for P2.
Stride length [m]	Accelerometer, Gyroscope	Walking	Distance between two non-consecutive initial contacts [16,24]
Walking speed [m/s]	Accelerometer, Gyroscope	Walking	Walking speed [16] during the test: $W\ speed = \frac{cadence}{60} * \frac{stride\ length}{2}$
Gait initiation [s]	Accelerometer, Gyroscope	In-between: Sit-to-Walk and Walking,	Time required to start walking after standing up
Max V, ML, AP [m/s^2], [°/s]	Accelerometer, Gyroscope	Sit-to-Walk, Turns, Turn-to-Sit	Maximum value of the signal along each respective axis
Range V, ML, AP [m/s^2], [°/s]	Accelerometer, Gyroscope	Sit-to-Walk, Turns, Turn-to-Sit	Range (max-min) of the signal along each respective axis
Mean V, ML, AP [m/s^2], [°/s]	Accelerometer, Gyroscope	Sit-to-Walk, Turns, Turn-to-Sit	Mean value of the signal along each respective axis
RMS AP, ML, V [m/s^2], [°/s]	Accelerometer, Gyroscope	Sit-to-Walk, Turns, Turn-to-Sit	Root Mean Square of the signal $RMS = \sqrt{\frac{1}{N}\sum_{i=1}^{N}(s_i - m)^2}$ where N is the total number of samples of the signal s, and m is the mean value.
NJS AP, ML, V [m]	Accelerometer	Sit-to-Walk, Turns, Turn-to-Sit	Time-Normalized Jerk Score [19] of the acceleration: $NJS = \sqrt{\frac{T^5}{2}\int_{T_{start}}^{T_{end}}(\dot{a})^2 dt}$ where T is the duration (T_{end}-T_{start}) of the considered subphase, and a is the acceleration measured in m/s².
NJS AP, ML, V [-]	Gyroscope	Sit-to-Walk, Turns, Turn-to-Sit	Normalized angular Jerk Score [19]: $NJS = \sqrt{\frac{T^5}{2\alpha^2}\int_{T_{start}}^{T_{end}}(\dot{\omega})^2 dt}$ where T is the turn duration (T_{end}-T_{start}) of the considered component, ω is the angular velocity in °/s, and α is the Turning Angle in °.
Angle V [°]	Gyroscope	Turns, Turn-to-Sit	Turning angle along the vertical axis. $V\ angle = \int_{T_{start}}^{T_{end}}\omega_V dt$ Where ω_V is the angular velocity along the vertical axis
Sit initiation [s]	Accelerometer, Gyroscope	Turn-to-Sit	Turn-to-Sit comprises two events, 'turn' and then 'sit'. TtS initiation measures the time required betweenending a turn andstart sitting

V = vertical, ML = medio-lateral, AP = antero-posterior

analyses. The normality of the kinematic parameters was tested using Shapiro-Wilk tests. Univariate analyses included the Kruskal-Wallis test and pairwise post-hoc analyses through the Dunn's test. The multivariate analysis evaluated a classifier's ability to use the kinematic features to discriminate between each cohort and healthy adults. We trained random forest classifiers based on recursive feature elimination, selecting the top 10 features, and validated them using a k-fold (k = 5) stratified cross-validation with 5 repetitions. Features were z-scored before classification to ensure consistency. Hyperparameters, including the number of estimators, were optimized using a grid search. Accuracy, F1-score, and the area under the receiver operating characteristic (ROC) curve (AUC) were used to evaluate the classifiers' performance.

Clinical concurrent validity was assessed by a linear correlation analysis between the kinematic features obtained from the L-test and relevant clinical scales specific to each cohort (Table IV). The iL-test kinematic features were also correlated with the Late Life Function and Disability Instrument (LLFDI - functional component) in the Mobilise-D cohorts. The correlations were quantified with Spearman's correlation coefficient.

Statistical significance was set at p < 0.05. All p-values were adjusted to control for multiple comparisons [25]. The statistical analyses were carried out using Python 3.8 with "scipy", "statsmodels", and "scikit_posthocs" libraries.

TABLE IV
CLINICAL SCALES DESCRIPTION

| Cohort	Clinical scale	Ranges
Congestive Heart Failure [CHF]	Kansas City Cardiomyopathy Questionnaire (KCCQ) [25]	0 (Poor) – 100 (Excellent)
Chronic Obstructive Pulmonary Disease [COPD]	Forced expiratory volume in one second, expressed as a percentage of the predicted norm (FEV-1) [26]	0 (Poor) – 100 (Excellent)
Multiple Sclerosis [MS]	The Expanded Disability Status Scale (EDSS) [27]	0 (No disability) - 10 (Death due to MS)
Parkinson's Disease [PD]	Movement Disorder Society Unified Parkinson's Disease Rating Scale Part III (MDS-UPDRS-III) [28]	0 (Excellent) – 132 (Poor)
Proximal- emoral Fracture [PFF]	The Short Physical Performance Battery (SPPB) [29]	0 (Poor) – 12 (Excellent)
Transfemoral Amputees [TFA]	The Amputee Mobility Predictor (AMP) [30]	0 (Poor) – 47 (Excellent)
All except TFA	Late Life Function and Disability Instrument (LLFDI) [31,32]	0 (Poor) – 100 (Excellent)
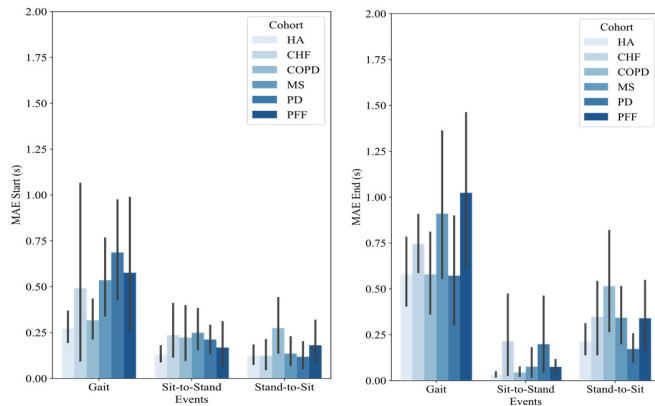
Fig. 4. Mean absolute error at the start and end of the segments.

III. RESULTS

A. iL-test Validation

The applied algorithms segmented all sub-phases within the L-test in all cohorts automatically. The four logical conditions, including the five sub-conditions for turns (Table II), were met for all participants of all cohorts. Two representative subjects of each cohort are shown in Supplementary Table 2 to illustrate the intermediate steps in the validation of sub-conditions for turns (C3).

When compared against stereophotogrammetry (the gold standard), the iL-test algorithm demonstrated very good segmentation performance. On average, mean absolute error for all cohorts were 0.2 seconds for postural transfers and 0.5 seconds for walking identification (Figure 4). The average Jaccard Index for all cohorts was 80% for postural transfers and 90% for the walking sub-phases.

B. Univariate Analysis

A total of 164 features were extracted, Shapiro-Wilk revealed a non-normal distribution of the features. The average L-test walking speed for HA was 1.0 m/s (sd = 0.2 m/s) with a stride length of 1.1 m (sd = 0.2 m). In contrast, transfemoral amputees (TFA) exhibited a reduced walking speed (0.6 m/s, sd = 0.2 m/s) and stride length (0.8 m, SD = 0.2 m). A table with reference values for all features and for each cohort can be found in Supplementary Table 3.

TABLE V
SIGNIFICANTLY DIFFERENT FEATURES
BETWEEN EACH COHORT AND HA

Cohort	total features	Significant features in each phase					
		W	StW	T1	T2	T3	TtS
CHF	6	0	0	2	3	1	0
COPD	1	0	0	0	0	1	0
MS	17	0	0	5	8	4	0
PD	16	0	0	0	5	6	5
PFF	35	1	2	7	9	12	4
TFA	68	7	3	12	16	15	15

The Kruskal-Wallis test indicated that 100 features were differentially distributed in at least one cohort. Afterwards, Dunn's test revealed that 88 characteristics differed significantly between clinical cohorts. Of the 88 characteristics, eleven were significant across at least ten cohort pairs (Supplementary Table 4).

TFA showed significantly reduced StW angular velocity ranges around the mediolateral (ML) axis when compared to the other cohorts. Walking speed and turn angles were greatly reduced in cohorts with more impaired mobility (PFF, TFA) (Figure 5).

Only one feature, the angle during the third turn (T3), was found to significantly differentiate between COPD and HA. Features derived from both 90° (T1, T3) and 180° (T2) turns were found to significantly differentiate participants with CHF, MS, and PD versus HA. Participants with PFF and TFA had the largest number of features (35 and 68 respectively) that significantly differentiated them versus HA and these features comprised all the sub-phases of the L-test (Table V).

C. Multivariate Analysis

Random forest classifiers were built to differentiate between each cohort and HA. Models for PFF and TFA exhibited an AUC over 90%, indicating substantial differences in mobility when compared to healthy adults. In contrast, models for CHF and COPD showed a performance near chance (Table VI, Supplementary Figure 1).

Models for MS and PD revealed moderate differences in mobility compared to healthy adults. Also, consistent with findings in univariate analysis, the model-selected features included a combination of features derived from the 90° and 180° turns. In addition to turn-derived features, walking-based features were found to be discriminative for PFF and TFA cohorts (Table VI).

D. Clinical Construct Validity

The clinical construct validity of the iL-test kinematic features was assessed by correlating them with clinical scales specific to each clinical cohort. The MS cohort revealed 18 features significantly correlated with the EDSS scale (T1: 1, T2: 6, TtS:11), with 12 having high correlations ($\rho > 0.7$) and 6 having moderate correlations ($\rho > 0.6$). A reduced movement range, longer duration, and higher jerk during turns were correlated with a higher EDSS score (deterioration of the
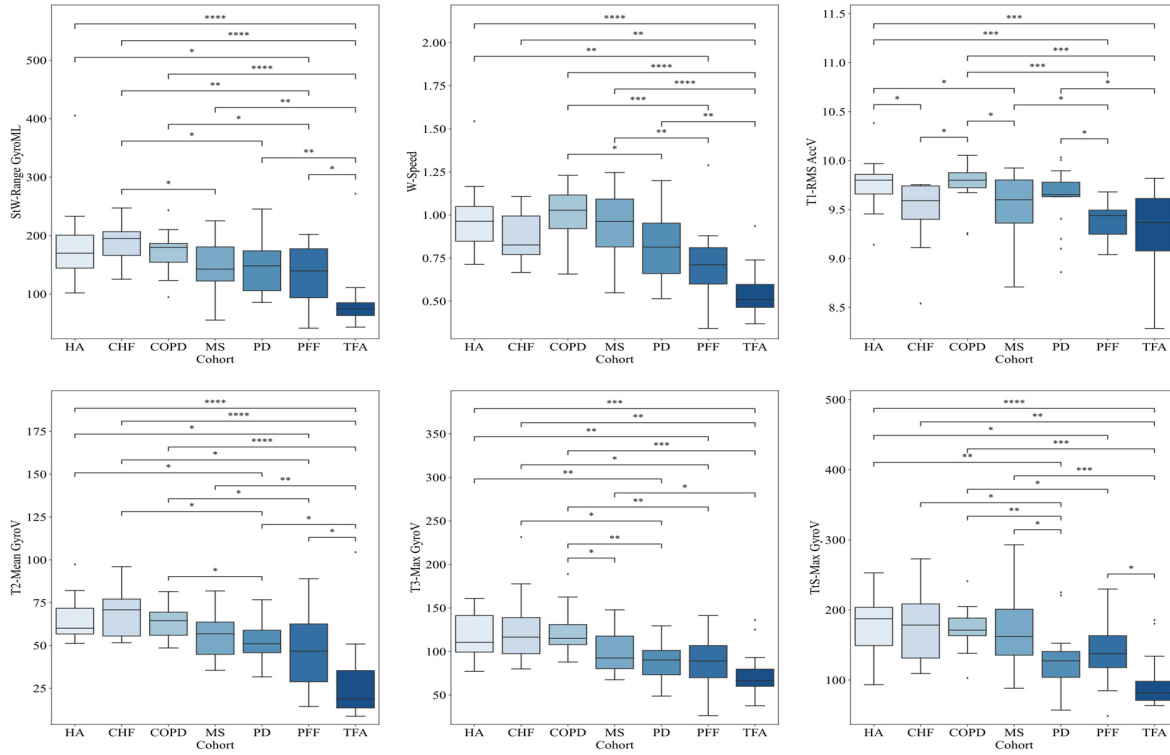
Fig. 5. Box plot with representative features for each segment. Significant differences are highlighted on top of the box plots (*: 1.00e-02 < p <= 5.00e-02, **: 1.00e-03 < p <= 1.00e-02, ***: 1.00e-04 < p <= 1.00e-03, ****: p <= 1.00e-04).

TABLE VI
MODEL PERFORMANCE METRICS

Cohort	Accuracy	F1 score	ROC AUC	Best Features
CHF	0.6±0.17	0.28±0.28	0.59±0.28	[StW-Duration, StW-NJS AccV, StW-NJS AccAP, T1-Max AccAP, T2-Max GyroAP, T2-Range GyroAP, TtS-V Angle, TtS-Range AccV, TtS-Max GyroML, TtS-Mean GyroML]
COPD	0.51±0.15	0.43±0.22	0.51±0.2	[StW-NJS GyroV, W-Stride Length, T1-Max GyroV, T1-Max GyroML, T1-Range GyroV, T2-Range GyroAP, T3-V Angle, T3-Range AccV, T3-Range AccAP, T3-Range GyroAP]
MS	0.71±0.17	0.69±0.19	0.83±0.14	[T1-Range GyroML, T1-Range GyroAP, T2-RMS AccV, T2-Range GyroAP, T2-NJS GyroV, T3-Max GyroML, T3-Range GyroML, T3-Mean GyroV, T3-RMS GyroV, TtS-Max AccAP]
PD	0.6±0.17	0.56±0.24	0.7±0.2	[StW-Mean GyroAP, StW-NJS GyroV, StW-NJS GyroAP, T2-Mean GyroV, T2-RMS GyroV, T2-NJS GyroV, T3-NJS AccML, T3-Mean GyroV, TtS-Range GyroV, TtS-NJS GyroV]
PFF	0.87±0.13	0.85±0.15	0.91±0.12	[W-Stride Length, W-Speed, T1-Max AccV, T1-Mean AccV, T1-RMS AccV, T2-Max AccV, T2-Mean AccV, T2-RMS AccV, T3-RMS AccV, T3-NJS AccML]
TFA	0.92±0.1	0.87±0.16	0.99±0.02	[W-Cadence, T1-Max AccV, T2-Mean GyroV, T2-NJS GyroV, TtS-Duration, TtS-NJS AccV, TtS-NJS AccML, TtS-Mean GyroV, TtS-NJS GyroV, TtS-Hesitation]

condition). Also, a worse condition was associated with longer and jerkier movements during the turn to sit (TtS).

For the PFF cohort, 59 features were significantly correlated with the SPPB score (StW:11, W:2, T1:5, T2:15, T3:13, TtS:13), with 28 having high correlations ($\rho > 0.7$) and 31 having moderate correlations ($\rho > 0.58$). Longer duration and jerkier transitions during a StW and TtS were associated with a lower SPPB score (deterioration of the condition). Also, a lower score was correlated with reduced movement ranges, longer duration, lower vertical angular velocity, higher jerk during turns, reduced walking speed, and shorter steps.

For the TFA cohort, 33 features were significantly correlated with the AMP score (W:1, T1:4, T2:8, T3:3, TtS:17), with

30 having high correlations ($\rho > 0.7$) and 3 having moderate correlations ($\rho > 0.67$). Longer duration, jerkier transitions, and reduced movement ranges during turns and turn-to-sit were associated with a lower AMP score (deterioration of the condition). Also, reduced walking speed was correlated with a lower score. No significant features were found to be correlated in the other cohorts. Supplementary figure 2 shows selected features for the cohorts that revealed significant correlations.

We further expanded the analysis by examining the LLFDI in the Mobilise-D cohorts. For the CHF cohort, 7 features were significantly correlated with the LLFDI score (StW:2, T2:5). Reduced medio-lateral angular velocity and higher jerk were associated with a lower LLFDI score (adverse outcome). Lower vertical angular velocity and jerkier movements during turns were also associated with a lower score. MS participants revealed two significant features in the TtS segment: the range and maximum value of the anteroposterior axis were positively correlated with LLFDI.

In PFF participants, 8 features showed significant correlations with the LLFDI score (StW:7, T2:1). Increased angular velocity range during T2 and longer duration and jerkier transitions in all the axes during StW were associated with a lower LLFDI score (lower functional level). After p-value adjustment for multiple comparisons, no significant correlations were found for HA, COPD, and PD cohorts, yet moderate correlations ($\rho \approx 0.6$) revealed similar trends, with lower walking speeds and shorter steps associated with a lower LLFDI. Reduced movement ranges, longer duration, and jerkier movements during turning and TtS were also

associated with a lower LLFDI score. Supplementary figure 3 shows selected features for the cohorts that revealed significant correlations. Two sub-components of the LLFDI score were also independently explored (basic lower extremity and advanced lower extremity) with similar results.

IV. DISCUSSION

This study introduces the instrumented L-test approach for comprehensive mobility assessment. The segmentation algorithm properly identified all the sub-phases comprised in the L-test in all cohorts. Subsequent technical validation against stereophotogrammetry revealed small errors and similar performance for postural transfers and gait identification as in previous instrumented mobility studies [6]. Here, we would like to remind readers of the nature of the multicohort study and highlight the power of this approach in the successful application of the instrumented L-test in severely compromised cohorts such as people with proximal femoral fractures and transfemoral amputees. This automated approach offers a promising solution to the limitations of manual assessments and the subjectivity inherent in such evaluations. The ability of the iL-test algorithm to accurately identify and segment activities within the L-test provides a strong foundation for future mobility assessments. With a low error, it offers objective results, essential in clinical practice. To confirm further the reliability of the segmentation algorithm, we randomly selected participants and visually inspected the correspondence of the acceleration signals and the stereophotogrammetry data with the automatic segmentation (Fig. 3). This visual verification served solely as an additional confirmation step and does not imply that human intervention is required for the proposed tool.

A total of 164 sensor-based features were extracted from all the L-test segmented events, with the selection of features guided by previously validated instrumented mobility tests (e.g., iTUG). The decision was made to keep most features used in the literature to ensure a comprehensive analysis of mobility in each cohort. In the univariate analysis, our findings emphasize the nuanced nature of kinematic differences observed during the L-test across various clinical cohorts. While only one feature, the angle during the third turn (T3), significantly differentiated COPD from HA, the picture was different for other cohorts. Participants with CHF (6 features), MS (17 features), and PD (16 features) displayed significant differences in features derived from both 90° (T1, T3) and 180° (T2) turns compared to healthy adults. The most distinctive patterns were observed in PFF (35 features) and TFA (68 features), highlighting the multifaceted kinematic distinctions characterizing these cohorts throughout the entire L-test sub-phases. The multivariate analysis confirmed these findings. The robust performance of the models for PFF and TFA, as indicated by AUC values exceeding 90%, underscores the effectiveness of these features in capturing substantial differences in mobility patterns when compared to healthy adults.

In contrast, the models built for CHF and COPD cohorts demonstrated performances near chance, suggesting no substantial mobility limitation (related to the L-Test functional

aspects) in these cohorts. The models for MS and PD cohorts revealed moderate differences in mobility compared to healthy adults, aligning with the patterns observed in the univariate analysis. A recursive feature elimination approach was applied to mitigate feature collinearity and enhance the interpretability of the selected models. Specific information on relevant features was found in sit-to-walk, walking, turning, and turn-to-sit segments in each cohort, as discussed in detail in the following sections.

A. Sit-to-Walk

In the PFF cohort, longer durations and jerkier transitions during Sit-to-Walk (StW) were associated with lower Short Physical Performance Battery (SPPB) scores and a lower Late Life Function and Disability Instrument (LLFDI) score. These findings suggest that individuals with proximal femoral fractures who exhibit prolonged and less fluid movements during postural transfers may experience compromised physical performance and functional abilities [26]. This observation aligns with common clinical experiences reported by individuals recovering from femoral fractures, where challenges in postural transitions and the associated dynamic aspects of movement are prevalent. Importantly, a low SPPB score has been shown to be a predictor of adverse clinical outcomes such as cognitive decline, falls, and death [27].

Parkinson's disease participants exhibited reduced StW angular velocity and higher jerk compared to healthy older adults, indicating the challenges these individuals face in initiating movement and maintaining smooth, controlled motion. Previous studies have hypothesized that the diminished ability to transition from sitting to standing observed in individuals with Parkinson's disease may originate from decreased hip flexion joint torque and an elongated duration for torque generation [28], [29].

Transfemoral amputees, on the other hand, showed significantly reduced StW angular velocity ranges around the mediolateral axis compared with all other cohorts. This result aligns with research indicating that transfemoral amputees often exhibit unique inter-joint coordination patterns, particularly at the hip joint, to compensate for the support-capability impairment due to limb amputation and to ensure foot placement accuracy [30], [31].

B. Walking

In the walking segment, distinct mobility patterns emerged for the proximal femoral fracture (PFF) and transfemoral amputee (TFA) cohorts. Reduced walking speed and stride length were evident in the PFF group compared to healthy adults (HA) and were associated with lower SPPB and LLFDI scores. This result suggests that individuals with proximal-femoral fractures who exhibit diminished walking speed and stride length may experience challenges in overall physical performance and functional abilities [32], [33].

Similarly, in the TFA cohort, walking speed and stride length were observed to be reduced compared to HA. Lower

walking speeds in the TFA group were also associated with a lower Amputee Mobility Predictor (AMP) score. These findings highlight the impact of reduced walking speed on the functional mobility of individuals with transfemoral amputation, emphasizing the importance of assessing and addressing gait parameters in this population. Studies have shown similar compensatory strategies, with amputees demonstrating altered gait parameters compared to non-disabled individuals [34], [35], [36].

C. Turns

In all the analyses performed, turns emerged as a prominent and consistent feature across all cohorts. The significant findings in univariate, multivariate, and clinical concurrent validity analyses notably highlighted the importance of turning dynamics. Turns encompassing 90° (T1, T3) and 180° (T2) rotations exhibited distinctive kinematic patterns crucial in distinguishing various clinical cohorts from healthy adults. In real-world scenarios, individuals often perform turns in various directions and angles, reflecting the complexity of everyday mobility. Studies have underscored the connections between turning strategies and factors such as fatigue, balance impairment, and geriatric syndromes such as increased risk of falling [37], [38], [39], [40], [41]. Our findings align with these studies, highlighting the significance of including both narrow and wide turns in mobility assessments to encompass a broader spectrum of real-world movement patterns.

In the MS cohort, reduced ranges in T2 and T3 vertical angles, coupled with increased jerk, signify notable differences in turning dynamics compared to healthy adults. These difficulties are often attributed to a combination of factors, including muscle weakness, spasticity, sensory deficits, and impaired central processing of motor commands. Specifically, the reduced ranges in T2 and T3 vertical angles observed in our study may reflect the altered postural control and coordination typically seen in MS during turns [42], [43], [44]. The correlation analysis with EDSS confirmed that a reduced movement range, longer duration, and higher jerk during turns were associated with a higher EDSS score (i.e., increased disability).

Similarly, individuals with PD exhibited reduced ranges in T2 and T3 vertical angles, along with increased jerk, indicating distinctive turning patterns. The reduced ranges in T2 and T3 vertical angles observed in our PD cohort during the L-test are consistent with previous studies reporting alterations in turning kinematics in PD [22], [45], [46], [47], [48], [49]. Individuals with PD often exhibit jerkier, smaller, and more segmented turns, commonly described as "en bloc" turning [50], which can be attributed to underlying motor deficits. Moreover, the literature supports the idea that turning deficits in PD are not solely related to motor symptoms but may also involve cognitive aspects. PD patients often experience difficulties in dual-tasking situations, and turning is considered a cognitively demanding task [51]. This cognitive-motor interaction can contribute to the observed alterations in turning dynamics.

In the PFF cohort, reduced T1, T2, and T3 vertical accelerations and increased T3 jerk were identified in univariate analysis, pointing to altered acceleration patterns during turns. These findings may stem from factors such as residual pain, muscle weakness, altered joint mechanics, or an adaptive gait strategy aimed at minimizing discomfort during turning activities [33], [52]. Also, the correlation analysis showed that longer durations, lower vertical angular velocity, and higher jerk during turns were associated with a lower SPPB score, indicating potential connections between impaired turning dynamics and physical performance in individuals with PFF.

For the TFA cohort, reduced T1 and T2 vertical angles, coupled with increased T2 jerk, suggest distinct kinematic patterns during turning. Furthermore, longer durations, jerkier transitions, and reduced movement ranges during turns were associated with a lower AMP score. These findings may be attributed to altered biomechanics due to limb loss. They could reflect the complex interplay between prosthetic use, residual limb function, and compensatory movements to navigate turning tasks effectively [53], [54]. Associations between turn-related features and the AMP score highlight the clinical relevance of turning dynamics in the context of amputee mobility.

In Dunn's test, reduced angles and ranges for all turns (T1, T2, and T3) were observed in the CHF cohort, suggesting altered kinematics during turning. Also, in COPD, a distinct reduction in T3 vertical angle was identified, indicating potential limitations in vertical angular movements during the third turn. However, in the multivariate analysis, these specific features did not exhibit discriminative power, suggesting that these cohorts did not show substantial mobility limitations in the iL-test.

The turn-to-sit phase revealed congruent results with previous postural and turning events (see supplementary materials). Considering the shared emphasis on turns in all cohorts, personalized rehabilitation interventions targeting turning movements could benefit individuals across clinical cohorts. Home-based exercise programs focusing on turning activities could empower individuals to improve their turning abilities independently, addressing unique mobility needs identified from different angles and directions.

Still, our study presents some limitations, including sample size impacting generalizability, influence of cohort severity on observed results, the absence of age-matched groups for direct comparisons, and the cross-sectional nature limiting longitudinal assessment. Differences in L-test path distances between the Mobilise-D and MOTU datasets (4m × 2m versus 7m × 3m) might have influenced certain outcomes. However, we mitigated this issue by excluding metrics directly sensitive to distance differences, such as walking duration and focused on distance-independent metrics such as turn and transfer durations.

Future studies should further validate these preliminary results in larger populations, include age-matched groups to better discriminate between cohorts and address potential confounding factors, explore subgroup analyses, longitudinal

changes, and integrate additional sensors for a more comprehensive understanding of movement patterns. Furthermore, the normalized jerk score might be correlated with the task's duration, so future studies should explore alternative smoothness metrics. Additionally, while this study emphasized speed, cadence, and stride length for their proven value in walking, as past studies showed, future studies could expand the repertoire with other walking-related metrics. Finally, comparative analyses with other mobility assessments, such as the Timed Up and Go (TUG) test, could provide deeper insights into digital mobility outcomes across diverse populations.

V. Conclusion

In conclusion, this study has validated the instrumented L-test automatic segmentation in seven cohorts, demonstrating its potential to foster mobility assessment across diverse clinical cohorts. The algorithms' accuracy in identifying and segmenting activities within the L-test offers an automatic objective tool for precise mobility assessment. The analysis of kinematic features as discriminators between clinical cohorts highlights the iL-test discriminative utility to provide nuanced insights into specific mobility characteristics, and supply hints for implementing personalized rehabilitative interventions.

This work advances the state of the art by introducing a novel mobility assessment tool that expands upon the currently used instrumented Timed Up and Go (iTUG) test. The inclusion of multiple turns, both 90° and 180°, highlights unique movement characteristics that are not captured by the TUG, emphasizing the importance of evaluating diverse turning movements. Additionally, the use of state-of-the-art algorithms ensures high accuracy in gait and activity segmentation. Finally, the multicohort framework, involving seven distinct clinical populations, underscores the versatility of the iL-test in addressing the mobility needs of various clinical conditions.

The significance of multiple turns, encompassing both 90° and 180° angles and different directions, emerged as a common theme across cohorts. These findings suggest that the iL-test, providing information about diverse activities such as turns, provides a promising, versatile platform for digital mobility assessment in various clinical populations. The findings presented here can serve as a foundation for future exploration, innovation, and the pursuit of more informed and individualized care for diverse clinical conditions.

Conflict of Interest

Acknowledgment

Jose Albites-Sanabria, Pierpaolo Palumbo, Ilaria D'Ascanio, Lucrezia Piraccini, Lorenzo Chiari, and Luca Palmerini are with the Department of Electrical, Electronic, and Information Engineering "Guglielmo Marconi," University of Bologna, 40136 Bologna, Italy (e-mail: jose.albitessanabri2@unibo.it).

Tecla Bonci is with the School of Mechanical, Aerospace and Civil Engineering and Insigneo Institute for in Silico Medicine, The University of Sheffield, S1 3JD Sheffield, U.K.

Marco Caruso, Francesca Salis, and Andrea Cereatti are with the Department of Electronics and Telecommunications, Politecnico di Torino, 10129 Turin, Italy.

Silvia Del Din and Lynn Rochester are with the Translational and Clinical Research Institute, Faculty of Medical Sciences, Newcastle University, NE2 4AE Newcastle upon Tyne, U.K., also with The National Institute for Health and Care Research (NIHR) Newcastle Biomedical Research Centre (BRC), Newcastle University, NE4 5PL Newcastle upon Tyne, U.K., and also with The Newcastle upon Tyne Hospitals NHS Foundation Trust, NE7 7DN Newcastle upon Tyne, U.K.

Lisa Alcock, Cameron Kirk, M. Encarna Micó-Amigo, and Kirsty Scott are with the Translational and Clinical Research Institute, Faculty of Medical Sciences, Newcastle University, NE2 4AE Newcastle upon Tyne, U.K.

Arne Kuederle is with the Machine Learning and Data Analytics Laboratory, Department of Artificial Intelligence in Biomedical Engineering, Friedrich-Alexander-Universität Erlangen-Nürnberg, 91054 Erlangen, Germany.

Anisoara Paraschiv-Ionescu is with the Laboratory of Movement Analysis and Measurement, École Polytechnique Fédérale de Lausanne, 1015 Lausanne, Switzerland.

Eran Gazit is with the Center for the Study of Movement, Cognition and Mobility, Neurological Institute, Tel Aviv Sourasky Medical Center, Tel Aviv 64239, Israel.

Felix Kluge and Arne Muller are with the Novartis Institutes of Biomedical Research, Novartis Pharma AG, 4056 Basel, Switzerland.

Clint Hansen and Walter Maetzler are with the Department of Neurology, University Medical Center Schleswig-Holstein, Campus Kiel, 24105 Kiel, Germany.

Jochen Klenk, Lars Schwickert, and Clemens Becker are with the Robert Bosch Gesellschaft für Medizinische Forschung, 70376 Stuttgart, Germany.

Dimitrios Megaritis and Ioannis Vogiatzis are with the Department of Sport, Exercise and Rehabilitation, Northumbria University Newcastle, NE7 7XA Newcastle upon Tyne, U.K.

Jeffrey M. Hausdorff is with the Center for the Study of Movement, Cognition, and Mobility, Neurological Institute, Tel Aviv Sourasky Medical Center, Tel Aviv 6997801, Israel, also with the Sagol School of Neuroscience and the Department of Physical Therapy, Faculty of Medical and Health Sciences, Tel Aviv University, Tel Aviv 6997801, Israel, and also with the Rush Alzheimer's Disease Center and the Department of Orthopaedic Surgery, Rush University Medical Center, Chicago, IL 60612 USA.

Brian Caulfield is with The Insight Centre for Data Analytics, University College Dublin, Dublin, D04 V1W8 Ireland, and also with the School of Public Health, Physiotherapy and Sports Science, University College Dublin, Dublin, D04 V1W8 Ireland.

Beatrix Vereijken is with the Department of Neuromedicine and Movement Science, Norwegian University of Science and Technology, 7491 Trondheim, Norway.

Claudia Mazzá is with the School of Mechanical, Aerospace and Civil Engineering and Insigneo Institute for in Silico Medicine, The University of Sheffield, S1 3JD Sheffield, U.K., and also with Indivi, Medical Science, 4051 Basel, Switzerland.

Ilaria Carpinella, Thomas Bowman, Roberta De Ciechi, Alessandro Torchio, Simona Bianchi, and Maurizio Ferrarin are with the IRCCS Fondazione Don Carlo Gnocchi, 20148 Milan, Italy.

Davide Cattaneo is with the IRCCS Fondazione Don Carlo Gnocchi, 20148 Milan, Italy, and also with the Department of Pathophysiology and Transplantation, University of Milan, 20100 Milan, Italy.

Pericle Randi is with the Unità operativa di medicina fisica e riabilitazione, INAIL Centro Protesi, Vigoroso di Budrio, 40054 Bologna, Emilia-Romagna, Italy. Angelo Davalli is with the Area ricerca e formazione, INAIL Centro Protesi, Vigoroso di Budrio, 40054 Bologna, Emilia-Romagna, Italy.

REFERENCES

[1] E. Pantelaki, E. Maggi, and D. Crotti, "Mobility impact and well-being in later life: A multidisciplinary systematic review," *Res. Transp. Econ.*, vol. 86, May 2021, Art. no. 100975, doi: 10.1016/j.retrec.2020.100975.

[2] C. H. Hirsch and A. Hategan, "Physiology and pathology of aging," in *Geriatric Psychiatry*. Cham, Switzerland: Springer, 2018, pp. 3–25.

[3] N. Salari, N. Darvishi, M. Ahmadipanah, S. Shohaimi, and M. Mohammadi, "Global prevalence of falls in the older adults: A comprehensive systematic review and meta-analysis," *J. Orthopaedic Surg. Res.*, vol. 17, no. 1, p. 334, Jun. 2022, doi: 10.1186/s13018-022-03222-1.

[4] R. W. Bohannon, "Reference values for the timed up and go test," *J. Geriatric Phys. Therapy*, vol. 29, no. 2, pp. 64–68, Aug. 2006, doi: 10.1519/00139143-200608000-00004.

[5] L. Montesinos, R. Castaldo, and L. Pecchia, "Wearable inertial sensors for fall risk assessment and prediction in older adults: A systematic review and meta-analysis," *IEEE Trans. Neural Syst. Rehabil. Eng.*, vol. 26, no. 3, pp. 573–582, Mar. 2018, doi: 10.1109/TNSRE.2017.2771383.

[6] P. Ortega-Bastidas, B. Gómez, P. Aqueveque, S. Luarte-Martínez, and R. Cano-de-la-Cuerda, "Instrumented timed up and go test (iTUG)—More than assessing time to predict falls: A systematic review," *Sensors*, vol. 23, no. 7, p. 3426, Mar. 2023, doi: 10.3390/s23073426.

[7] M. Mancini, K. Smulders, R. G. Cohen, F. B. Horak, N. Giladi, and J. G. Nutt, "The clinical significance of freezing while turning in Parkinson's disease," *Neuroscience*, vol. 343, pp. 222–228, Feb. 2017, doi: 10.1016/j.neuroscience.2016.11.045.

[8] A. B. Deathe and W. C. Miller, "The l test of functional mobility: Measurement properties of a modified version of the timed 'Up & Go' test designed for people with lower-limb amputations," *Phys. Therapy*, vol. 85, no. 7, pp. 626–635, Jul. 2005, doi: 10.1093/ptj/85.7.626.

[9] E. Yuksel, M. Eymir, B. Unver, and V. Karatosun, "Reliability, concurrent validity and minimal detectable change of the l test in patients with total knee arthroplasty," *Disability Rehabil.*, vol. 44, no. 14, pp. 3714–3718, Jul. 2022, doi: 10.1080/09638288.2021.1871670.

[10] J. S. Kim, D. Y. Chu, and H. S. Jeon, "Reliability and validity of the l test in participants with chronic stroke," *Physiotherapy*, vol. 101, no. 2, pp. 161–165, Jun. 2015, doi: 10.1016/j.physio.2014.09.003.

[11] A. Nalbant, B. Unver, and V. Karatosun, "Test–retest reliability of the L-Test in patients with advanced knee osteoarthritis," *Physiotherapy Theory Pract.*, vol. 38, no. 13, pp. 2983–2987, Nov. 2022, doi: 10.1080/09593985.2021.1967539.

[12] B. Haas, E. Clarke, L. Elver, E. Gowman, E. Mortimer, and E. Byrd, "The reliability and validity of the L-test in people with Parkinson's disease," *Physiotherapy*, vol. 105, no. 1, pp. 84–89, Mar. 2019, doi: 10.1016/j.physio.2017.11.218.

[13] A. L. McCreath Frangakis, E. D. Lemaire, and N. Baddour, "Subtask segmentation methods of the timed up and go test and l test using inertial measurement Units—A scoping review," *Information*, vol. 14, no. 2, p. 127, Feb. 2023, doi: 10.3390/info14020127.

[14] L. Palmerini et al., "Mobility recorded by wearable devices and gold standards: The Mobilise-D procedure for data standardization," *Scientific Data*, vol. 10, no. 1, pp. 1–38, Jan. 2023, doi: 10.1038/s41597-023-01930-9.

[15] C. Mazza et al., "Technical validation of real-world monitoring of gait: A multicentric observational study," *BMJ Open*, vol. 11, no. 12, Dec. 2021, Art. no. e050785, doi: 10.1136/bmjopen-2021-050785.

[16] L. Rochester et al., "A roadmap to inform development, validation and approval of digital mobility outcomes: The Mobilise-D approach," *Digit. Biomarkers*, vol. 4, no. 1, pp. 13–27, Jan. 2021, doi: 10.1159/000512513.

[17] L. Adamowicz et al., "Assessment of sit-to-stand transfers during daily life using an accelerometer on the lower back," *Sensors*, vol. 20, no. 22, p. 6618, Nov. 2020, doi: 10.3390/s20226618.

[18] M. El-Gohary et al., "Continuous monitoring of turning in patients with movement disability," *Sensors*, vol. 14, no. 1, pp. 356–369, Dec. 2013, doi: 10.3390/s140100356.

[19] M. E. Micó-Amigo et al., "Assessing real-world gait with digital technology? Validation, insights and recommendations from the Mobilise-D consortium," *J. NeuroEngineering Rehabil.*, vol. 20, no. 1, pp. 1–78, Jun. 2023, doi: 10.1186/s12984-023-01198-5.

[20] T. Bonci et al., "An algorithm for accurate marker-based gait event detection in healthy and pathological populations during complex motor tasks," *Frontiers Bioengineering Biotechnol.*, vol. 10, pp. 1–15, Jun. 2022, doi: 10.3389/fbioe.2022.868928.

[21] J. M. Hancock, "Distance (Jaccard Index, Jaccard Similarity Coefficient)," in *Dictionary of Bioinformatics and Computational Biology*. Hoboken, NJ, USA: Wiley, 2004.

[22] L. Palmerini, S. Mellone, G. Avanzolini, F. Valzania, and L. Chiari, "Quantification of motor impairment in Parkinson's disease using an instrumented timed up and go test," *IEEE Trans. Neural Syst. Rehabil. Eng.*, vol. 21, no. 4, pp. 664–673, Jul. 2013, doi: 10.1109/TNSRE.2012.2236577.

[23] A. Weiss et al., "Can an accelerometer enhance the utility of the timed up & go test when evaluating patients with Parkinson's disease?" *Med. Eng. Phys.*, vol. 32, no. 2, pp. 119–125, Mar. 2010, doi: 10.1016/j.medengphy.2009.10.015.

[24] A. Coni et al., "Comparison of standard clinical and instrumented physical performance tests in discriminating functional status of high-functioning people aged 61–70 years old," *Sensors*, vol. 19, no. 3, p. 449, Jan. 2019, doi: 10.3390/s19030449.

[25] Y. Benjamini, A. M. Krieger, and D. Yekutieli, "Adaptive linear step-up procedures that control the false discovery rate," *Biometrika*, vol. 93, no. 3, pp. 491–507, Sep. 2006, doi: 10.1093/biomet/93.3.491.

[26] S. E. Lamb, R. E. Morse, and J. G. Evans, "Mobility after proximal femoral fracture: The relevance of leg extensor power, postural sway and other factors," *Age Ageing*, vol. 24, no. 4, pp. 308–314, 1995, doi: 10.1093/ageing/24.4.308.

[27] F. Lauretani et al., "Short-physical performance battery (SPPB) score is associated with falls in older outpatients," *Aging Clin. Experim. Res.*, vol. 31, no. 10, pp. 1435–1442, Oct. 2019, doi: 10.1007/s40520-018-1082-y.

[28] Y. R. Fatmehsari and F. Bahrami, "Sit-to-stand or stand-to-sit: Which movement can classify better parkinsonian patients from healthy elderly subjects?" in *Proc. 18th Iranian Conf. Biomed. Eng. (ICBME)*, Dec. 2011, pp. 48–53.

[29] M. K. Y. Mak, O. Levin, J. Mizrahi, and C. W. Y. Hui-Chan, "Joint torques during sit-to-stand in healthy subjects and people with Parkinson's disease," *Clin. Biomechanics*, vol. 18, no. 3, pp. 197–206, Mar. 2003.

[30] Z. Xu et al., "Lower limb inter-joint coordination of unilateral trans-femoral amputees: Implications for adaptation control," *Appl. Sci.*, vol. 10, no. 12, p. 4072, Jun. 2020, doi: 10.3390/app10124072.

[31] H. Burger, J. Kuželicki, and C. Marincek, "Transition from sitting to standing after trans-femoral amputation," *Prosthetics Orthotics Int.*, vol. 29, no. 2, pp. 139–151, Aug. 2005, doi: 10.1080/03093640500199612.

[32] D. Bai et al., "Effect of types of proximal femoral fractures on physical function such as lower limb function and activities of daily living," *Phys. Therapy Res.*, vol. 24, no. 1, pp. 24–28, Apr. 2021, doi: 10.1298/ptr.e10050.

[33] M. Galler, M. Zellner, C. Roll, C. Bäuml, B. Fuchtmeier, and F. Muller, "A prospective study with ten years follow-up of two-hundred patients with proximal femoral fracture," *Injury*, vol. 49, no. 4, pp. 841–845, Apr. 2018, doi: 10.1016/j.injury.2018.02.026.

[34] Z. Aftab and R. Shad, "Estimation of gait parameters using leg velocity for amputee population," *PLoS ONE*, vol. 17, no. 5, May 2022, Art. no. e0266726, doi: 10.1371/journal.pone.0266726.

[35] J. J. Genin, G. J. Bastien, B. Franck, C. Detrembleur, and P. A. Willems, "Effect of speed on the energy cost of walking in unilateral traumatic lower limb amputees," *Eur. J. Appl. Physiol.*, vol. 103, no. 6, pp. 655–663, Aug. 2008, doi: 10.1007/s00421-008-0764-0.

[36] A. M. Boonstra, V. Fidler, and W. H. Eisma, "Walking speed of normal subjects and amputees," *Prosthetics Orthotics Int.*, vol. 17, no. 2, pp. 78–82, Aug. 1993, doi: 10.3109/03093649309164360.

[37] M. Justine, H. Manaf, A. Sulaiman, S. Razi, and H. A. Alias, "Sharp turning and corner turning: Comparison of energy expenditure, gait parameters, and level of fatigue among community-dwelling elderly," *Bio. Med. Res. Int.*, vol. 2014, pp. 1–6, May 2014.

[38] R. L. Wright, D. M. Peters, P. D. Robinson, A. J. Sitch, T. N. Watt, and M. A. Hollands, "Differences in axial segment reorientation during standing turns predict multiple falls in older adults," *Gait Posture*, vol. 36, no. 3, pp. 541–545, Jul. 2012, doi: 10.1016/j.gaitpost.2012.05.013.

[39] J. Albites-Sanabria, P. Palumbo, S. Bandinelli, L. Palmerini, and L. Chiari, "Fall risk assessment using wearable-based turn detection: Comparison of different algorithms during real-world monitoring," in *Proc. 16th Int. Joint Conf. Biomed. Eng. Syst. Technol.*, 2023, pp. 294–300.

[40] J. M. Leach, S. Mellone, P. Palumbo, S. Bandinelli, and L. Chiari, "Natural turn measures predict recurrent falls in community-dwelling older adults: A longitudinal cohort study," *Sci. Rep.*, vol. 8, no. 1, p. 4316, Mar. 2018, doi: 10.1038/s41598-018-22492-6.

[41] J. Albites-Sanabria et al., "Real-world balance assessment while standing for fall prediction in older adults," *IEEE Trans. Biomed. Eng.*, vol. 71, no. 3, pp. 1076–1083, Mar. 2024, doi: 10.1109/tbme.2023.3326306.

[42] V. V. Shah et al., "Quantity and quality of gait and turning in people with multiple sclerosis, Parkinson's disease and matched controls during daily living," *J. Neurol.*, vol. 267, no. 4, pp. 1188–1196, Apr. 2020, doi: 10.1007/s00415-020-09696-5.

[43] G. Adusumilli et al., "Turning is an important marker of balance confidence and walking limitation in persons with multiple sclerosis," *PLoS ONE*, vol. 13, no. 6, Jun. 2018, Art. no. e0198178, doi: 10.1371/journal.pone.0198178.

[44] L. Weed, C. Little, S. L. Kasser, and R. S. McGinnis, "A preliminary investigation of the effects of obstacle negotiation and turning on gait variability in adults with multiple sclerosis," *Sensors*, vol. 21, no. 17, p. 5806, Aug. 2021, doi: 10.3390/s21175806.

[45] P.-Y. Chou and S.-C. Lee, "Turning deficits in people with Parkinson's disease," *Tzu Chi Med. J.*, vol. 25, no. 4, pp. 200–202, Dec. 2013, doi: 10.1016/j.tcmj.2013.06.003.

[46] L. Palmerini, "Identification of characteristic motor patterns preceding freezing of gait in Parkinson's disease using wearable sensors," *Front. Neurol.*, vol. 8, pp. 1–15, May 2017.

[47] L. Brognara, P. Palumbo, B. Grimm, and L. Palmerini, "Assessing gait in Parkinson's disease using wearable motion sensors: A systematic review," *Diseases*, vol. 7, no. 1, p. 18, Feb. 2019, doi: 10.3390/diseases7010018.

[48] T. Herman, A. Weiss, M. Brozgol, N. Giladi, and J. M. Hausdorff, "Identifying axial and cognitive correlates in patients with Parkinson's disease motor subtype using the instrumented timed up and go," *Exp. Brain Res.*, vol. 232, no. 2, pp. 713–721, Feb. 2014, doi: 10.1007/s00221-013-3778-8.

[49] A. Weiss et al., "The transition between turning and sitting in patients with Parkinson's disease: A wearable device detects an unexpected sequence of events," *Gait Posture*, vol. 67, pp. 224–229, Jan. 2019, doi: 10.1016/j.gaitpost.2018.10.018.

[50] S. Akram, J. S. Frank, and M. Jog, "Parkinson's disease and segmental coordination during turning: I. standing turns," *Can. J. Neurological Sci. J. Canadien des Sci. Neurologiques*, vol. 40, no. 4, pp. 512–519, Jul. 2013, doi: 10.1017/s0317167100014591.

[51] R. Vitorio et al., "Dual-task costs of quantitative gait parameters while walking and turning in people with Parkinson's disease: Beyond gait speed," *J. Parkinson's Disease*, vol. 11, no. 2, pp. 653–664, Apr. 2021, doi: 10.3233/jpd-202289.

[52] R. Bajracharya, J. M. Guralnik, M. D. Shardell, M. C. Hochberg, D. L. Orwig, and J. S. Magaziner, "Predictors of mobility status one year post hip fracture among community-dwelling older adults prior to fracture: A prospective cohort study," *J. Amer. Geriatrics Soc.*, vol. 71, no. 8, pp. 2441–2450, Aug. 2023, doi: 10.1111/jgs.18327.

[53] S. M. Clemens et al., "Temporal-spatial values during a 180° step turn in people with unilateral lower limb amputation," *Gait Posture*, vol. 63, pp. 276–281, Jun. 2018, doi: 10.1016/j.gaitpost.2018.05.016.

[54] E. C. Prinsen, M. J. Nederhand, and J. S. Rietman, "Adaptation strategies of the lower extremities of patients with a transtibial or transfemoral amputation during level walking: A systematic review," *Arch. Phys. Med. Rehabil.*, vol. 92, no. 8, pp. 1311–1325, Aug. 2011, doi: 10.1016/j.apmr.2011.01.017.